ISSN 0965-5441, Petroleum Chemistry, 2017, Vol. 57, No. 12, pp. 1043–1051. © Pleiades Publishing, Ltd., 2017.
Original Russian Text © M.V. Magomedova, E.G. Peresypkina, I.A. Davydov, S.N. Khadzhiev, 2017, published in Neftekhimiya, 2017, Vol. 57, No. 6, pp. 663–671.

Olefin Synthesis from Dimethyl Ether in the Presence of a Hydrothermally Treated Mg–HZSM-5/Al_2O_3 Catalyst: Effect of Reaction Conditions on the Product Composition and Ratio

M. V. Magomedova, E. G. Peresypkina*, I. A. Davydov, and S. N. Khadzhiev
Topchiev Institute of Petrochemical Synthesis, Russian Academy of Sciences, Moscow, Russia
**e-mail: peresypkina_eg@ips.ac.ru*

Received September 12, 2017

Abstract—Systematic studies of olefin synthesis from dimethyl ether (DME) in the presence of a hydrothermally treated HZSM-5 zeolite catalyst modified with magnesium have been conducted. Dependences of DME conversion, product yield and selectivity, and lower olefin ratio on space time in the temperature range of 320–360°C have been analyzed. The type of the resulting products has been determined, and assumptions about the reaction chemistry have been made to reveal the role of methylation and hydrogen-transfer reactions in the products formation.

Keywords: olefin synthesis, dimethyl ether, HZSM-5 zeolite, chemistry, kinetics
DOI: 10.1134/S0965544117100115

To date, olefin synthesis from methanol and/or dimethyl ether (DME) has been extensively studied: various theories on the reaction and formation of the first C–C bond mechanism have been put forward [1–3]; the secondary reactions of the C_2–C_4 olefins conversion—the methylation of ethylene, propylene, *n*-butene, pentene [4–8], and aromatic compounds with methanol [5, 9, 10] and the methylation of olefins with DME [11, 12]—have been studied; routes for the transition states of isomerization, cracking, and hydrogen transfer formation have been proposed [13–16]; the kinetics has been studied in detail [17–20].

Most of the authors assume that the first stage is methanol dehydration to DME; this reaction occurs at a significantly higher rate than the rate of olefin production steps and has a high enthalpy of −184 kcal/kg (methanol) [21]. In this aspect, all other products, except for DME, are formed during secondary reactions. This concept has given rise to the development of methanol-to-olefins (MTO) technologies wich include two reactors—one is for methanol conversion to DME by dehydration, and the second one to olefins synthesis. This principle has been implemented in the following commercial processes using HZSM-5 zeolites: the MTP technology (Lurgi, Germany) and the DTP technology (Japan Gasoline Company and Mitsubishi Chemical, Japan).

However, since the 2000s, close attention has been paid to the study of olefin synthesis using DME as a feedstock produced directly from synthesis gas [11, 22–28]. According to experiments of the cited authors, the main products are C_2–C_4 olefins, higher C_5–C_8 olefins, C_1–C_8 alkanes, and aromatic compounds. The methanol formation as a by-product is attributed with the DME reversible hydration reaction [29] or the DME chemisorption on a zeolite surface to form methanol and methoxy groups [27].

Almost all of the reported in literature research results was received using fresh zeolite catalysts samples and do not take into account the possibility of significantly changing their properties under commercial operation conditions. In a number of studies over HZSM-5-based catalysts [30–32], it was shown that, under olefin synthesis conditions, these catalysts quite rapidly lose their initial activity and selectivity; the zeolite deactivation is associated with a change in acidity caused by the blocking of the active sites by the coke. These results show that studies should be conducted in the presence of catalyst samples exhibiting properties that are similar to those expected in a long-term commercial use, i.e., artificially aged samples.

A well-known method of catalyst aging is a high-temperature steam treatment. A review of the literature shows that extensive studies of zeolite dealumination via steam treatment are mostly focused on changes in the structural and acidic properties of the material [33–35]. However, studies of the reaction chemical aspects in the presence of a steam-treated catalyst have not been reported.

In this context, analysis of the reaction conditions effect on the product composition and ratio in the presence of a hydrothermal treated catalyst is relevant for the industrial process of olefin synthesis from DME; this study is focused on the problem.

EXPERIMENTAL

A magnesium-containing catalyst was synthesized at the pilot factory using a ZSM-5 type zeolite with a SiO_2/Al_2O_3 ratio of 37, which is supplied in the ammonium form (Angarsk catalyst and organic synthesis plant). The zeolite was mixed with an alumina suspension with an Al_2O_3 content of 23 wt % in terms of dry residue (Promyshlennye Katalizatory); after that, extrudates were formed (Al_2O_3 content in the finished catalyst of 33–34 wt %) and calcined at 500°C for 4 h. To introduce a required amount of magnesium (1.0 wt %), the prepared pellets were impregnated with an aqueous solution of magnesium nitrate at room temperature for 24 h and then dried at 110°C and calcined at 500°C for 4 h. The steam treatment of the catalyst was conducted at 500°C for 6 h (stabilization) using the equipment and procedure described in [25]. After high-temperature steam treatment, the crystalline phase content in the zeolite structure remained almost unchanged (Table 1). The observed changes in the structural and acidic properties of the catalyst are consistent with the literature data [36, 37].

The mechanisms of olefin synthesis from DME were studied on a laboratory unit in the flow mode in the temperature range of 320–360°C at atmospheric pressure. The reactor was a quartz tube with an internal diameter of 10 mm; it was equipped with a central well for a movable thermocouple with a diameter of 4 mm to measure the temperature directly in the catalyst bed. The reactor was heated using an electric furnace; temperature in the furnace was set using a TRM-210 regulator (Russia). The catalyst charge was 0.5–1.0 g (0.4–0.63 mm fraction). Before loading into the thermal comfort zone of the reactor, a catalyst sample was mixed with quartz in a volume ratio of 1 : 1. To heat the feed, the upper part of the reactor space was filled with a quartz.

Table 1. X-ray diffraction analysis of the crystalline phase content in the zeolite component

Catalyst	Crystallinity, %
Mg–HZSM-5/Al_2O_3	93
Steamed Mg–HZSM-5/Al_2O_3	92

A mixture of DME (amount, 99.99 wt %; manufacturer, Akzo Nobel, the Netherlands) with nitrogen was used as a feedstock in the experiments. The DME concentration in the mixture with nitrogen was 10–13 vol %.

In olefin synthesis, space time per DME carbon was varied in a range of 0.2–3.2 g_{cat} h/g_C to provide the DME conversion in a range of 20–95%.

Reaction product selectivity and yield were calculated without taking into account the resulting water according to the equations

$$S_i = \frac{n_{Ci}}{\sum n_{Ci...n}}, \text{ mol \%}$$

$$Y_i = \frac{n_{Ci}}{n_{DME(feed)}}, \text{ mol\%},$$

where n_{Ci} is the moles number of carbon-containing compound i, mol/h; $i...n$ is the carbon-containing products; and $n_{DME(feed)}$ is the number of DME moles, mol/h.

Analysis of reaction products was conducted using a Kristallyuks-4000M on-line gas chromatograph equipped with a flame ionization detector and a thermal conductivity detector. The composition of C_1–C_7 hydrocarbons, methanol, and DME was determined on a 27.5 m × 0.32 mm × 10 μm capillary column with a CP-Poraplot Q phase. Nitrogen was determined on a 3.0 m × 4 mm × 3 mm packed column with a Porapak Q phase. Analysis was conducted using temperature programming of 90–250°C and helium as a carrier gas. The chromatograms were processed using the NetChromWin software.

RESULTS AND DISCUSSION

Effect of Temperature and Space Time

Data on the DME conversion in a temperature range of 320–360°C at a space time of 0.2–3.2 g_{cat} h/g_C in the presence of a stabilized Mg–HZSM-5/Al_2O_3 catalyst sample are shown in Fig. 1. An increase in temperature leads to a significant increase in the conversion rate of DME. The initial section of the “conversion–space time” dependence is linear; this behavior is most probably attributed to the first order with respect to DME concentration in the equation for DME consumption rate.

Dependences of the product yield on the contact time at temperatures of 320 and 360°C are shown in Figs. 2, 4, and 5. It is evident that the stabilized Mg–HZSM-5/Al_2O_3 catalyst sample provides a high methanol content in the products; the dependence of methanol yield on space time has an extremum (Fig. 2,

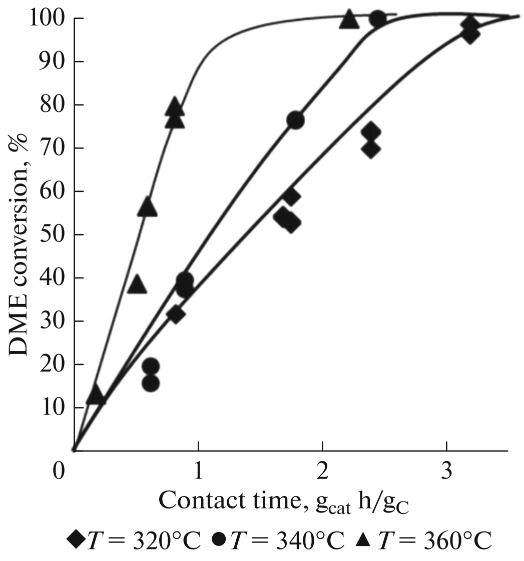

Fig. 1. The DME conversion vs space time for a stabilized Mg–HZSM-5/Al_2O_3 catalyst.

solid line). An increase in temperature leads to a shift of the extremum toward shorter space times. It should be noted that the highest methanol yield is 27–32 mol %; this value is significantly higher than the equilibrium yield (Fig. 3, dash-and-dot line) calculated on the assumption that DME is converted to olefins and water and the resulting water is involved in the hydration of the remaining (unreacted) DME.

The propylene yield exhibits an extreme behavior similar to that of methanol (Fig. 2, dashed line); as in the case of methanol, the temperature increasing leads to a shift of the propylene yield maximum to the shorter space times.

The dependences of the ethylene, butenes, C_1–C_4 alkanes, and C_5–C_7 hydrocarbons yields exhibit quite a different behavior (Figs. 4, 5). It is evident that, with an increase in the space time, the ethylene and butenes yield increases monotonically, while the yield of C_1–C_4 alkanes and C_5–C_7 hydrocarbons increases nonlinearly (Fig. 5).

The formation of C_1–C_4 alkanes and C_5–C_7 hydrocarbons, which are secondary products, as in catalytic cracking [38], largely occurs involving hydrogen transfer reactions:

Alkene + Alkene → Alkane + Diene;
Alkene + Alkene → Cycloalkane;

Diene + Alkene → Alkane + Arene;
ΣDiene → Arene +H_2;

Cycloalkane + Alkene → Alkane + Arene.

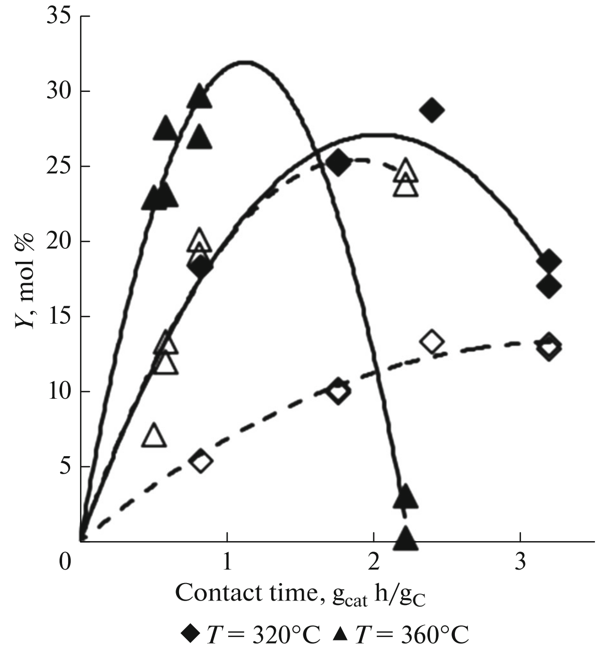

Fig. 2. The methanol yield (solid line) and propylene yield (dashed line) VS contact time at the different temperatures.

An increase in temperature from 320 to 360°C leads to a change in the behavior of formation of C_1–C_4 alkanes and C_5–C_7 hydrocarbons. The behavior of the curves corresponds to the apparent dependences for the final products at the low temperature and for

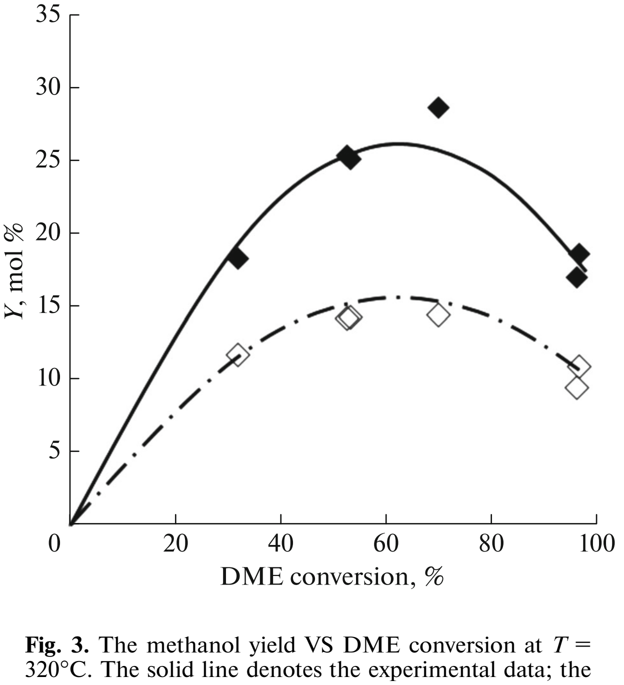

Fig. 3. The methanol yield VS DME conversion at T = 320°C. The solid line denotes the experimental data; the dash-and-dot line stands for the calculated equilibrium.

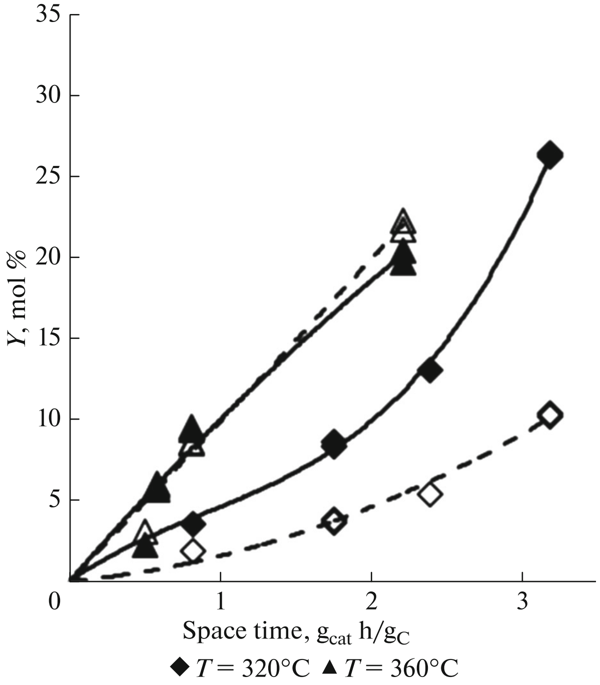

Fig. 4. The ethylene yield (solid line) and butenes yield (dashed line) VS contact time at the different temperatures.

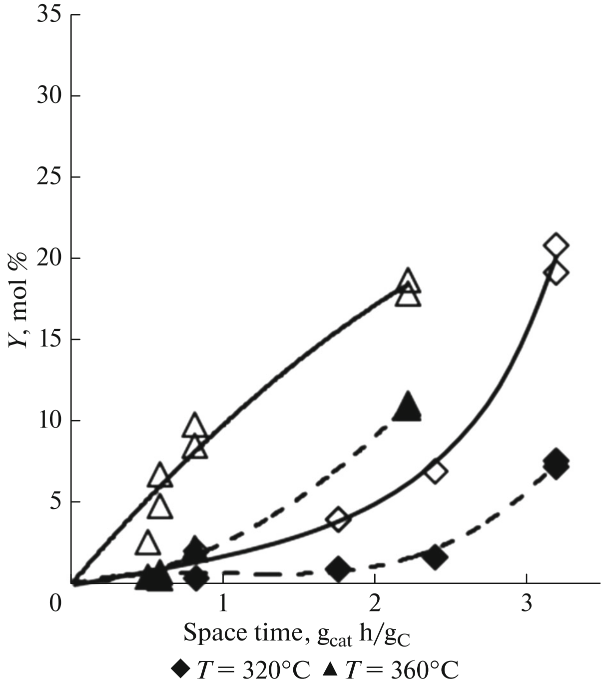

Fig. 5. The C_1–C_4 alkanes yield (dashed line) and C_5–C_7 hydrocarbons yield (solid line) VS contact time at the different temperatures.

the intermediate products at the higher temperature; this relationship is most pronounced for butenes and C_5–C_7 hydrocarbons.

Note that the behavior of the ethylene yield varies only slightly with increasing temperature; this is seems seems to the lower reactivity of ethylene in comparison with other hydrocarbons, wich was reported also in [27, 28].

The apparent dependences for the product yield are consistent with the results [29] describing a kinetic model and dependences of the product mole fractions of the products on space time at temperatures of 325–400°C in the presence of an HZSM-5 zeolite with a high silica ratio ($SiO_2/Al_2O_3 = 280$) for the initial catalyst activity conditions—at zero time on stream.

Analysis of our data reveals features that have not been previously observed in similar studies of oxygenate conversion, in particular, the maximum yield of methanol and propylene (in mole fractions) as a function of space time.

Perez-Uriarte et al. [29] attribute the methanol formation with the DME hydration reaction in the system; however, our calculations based on the amount of water in the system give significantly lower equilibrium methanol yields. It seems, there is another pathway of methanol formation which leads to the observed yield; which is not associated with DME hydration reaction.

The nonmonotonic propylene yield behavior was supposed in [28] to be due to the high reactivity one in oligomerization–cracking reactions with ethylene and butenes producing. However, this assumption explains neither the observed correlation of the propylene and methanol yields nor the extremum absence in the curve of the butene yield, although the butenes cracking occurs more vigorously than propylene.

The data obtained by measuring the product yield as a function of space time lead to the following conclusions: both methanol and propylene are intermediate products of the reaction; C_1–C_4 alkanes are final products; and ethylene, butenes, and C_5–C_7 hydrocarbons change their behavior with temperature and can be either final (at $T = 320$–340°C) or intermediate products (at $T > 360$°C).

To reveal the product formation sequence (primary/secondary), dependences of product selectivity via DME conversion at the different temperatures were plotted (Figs. 6–8) and values corresponding to DME zero conversion were determined.

The data show that the methanol selectivity as a function of DME conversion linearly decreases and hardly depends on the reaction temperature (Fig. 6a). Extrapolation of the line to the zero DME conversion value gives a methanol selectivity of about 75–78 mol %. This finding suggests that methanol is a primary product of the reaction.

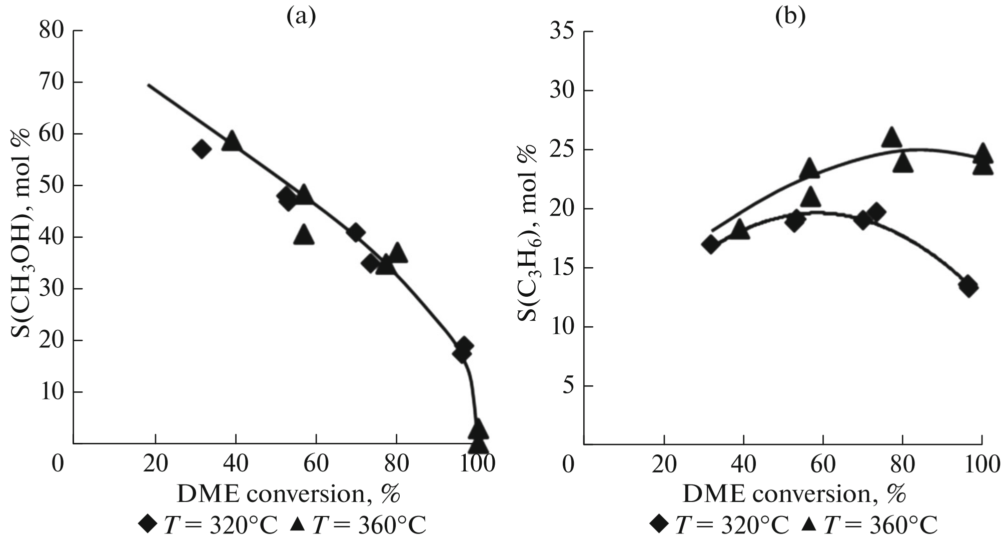

Fig. 6. The selectivity of methanol (a) and propylene (b) formation VS DME conversion at the different temperatures.

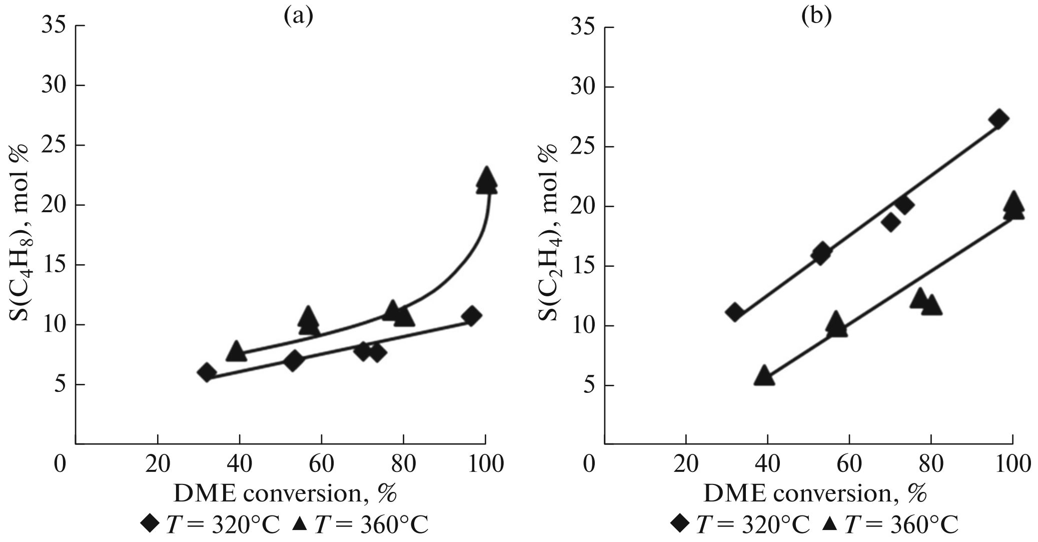

Fig. 7. The selectivity of butenes (a) and ethylene (b) formation VS DME conversion at the different temperatures.

Along with methanol, the primary products with a nonzero selectivity at a zero space time undoubtedly include propylene, butenes, and C_5–C_7 hydrocarbons (Figs. 6b, 7a, 8) with apparent molar selectivities of 75–78, 11–13, and 4–5 mol %, respectively. Ethylene is a primary product at the low reaction temperature and a secondary product at the high temperature (Fig. 7b). Unlike selectivities for other reaction products, the ethylene selectivity decreases with increasing temperature; this finding is an unexpected result. C_1–C_4 alkanes undoubtedly are secondary products of the reaction.

This result is inconsistent with the literature concepts of ethylene as the main primary product of oxygenate conversion. Propylene was identified as a primary product only in [27] in IR spectroscopy studies in a temperature range of 200–250°C. Most probably, ethylene is the main primary product only in the case of methanol conversion and the mechanism details of the methanol and DME conversion to olefins differ.

It is noteworthy that in a DME conversion range above 70–75%, the selectivity for propylene passes through a maximum (Fig. 6b) and the selectivity for butenes and C_1–C_4 alkanes abruptly increases (Figs. 7a, 8). This behavior is most likely due to both

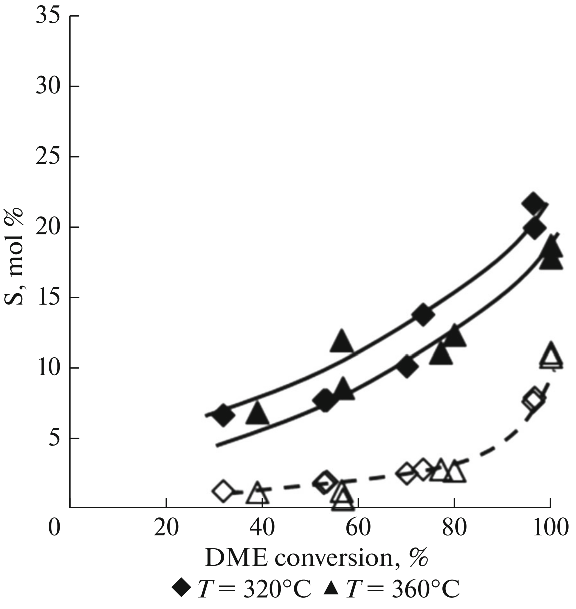

Fig. 8. The selectivity of C_1–C_4 alkanes (dashed line) and C_5–C_7 hydrocarbons (solid line) production VS DME conversion at the different temperatures.

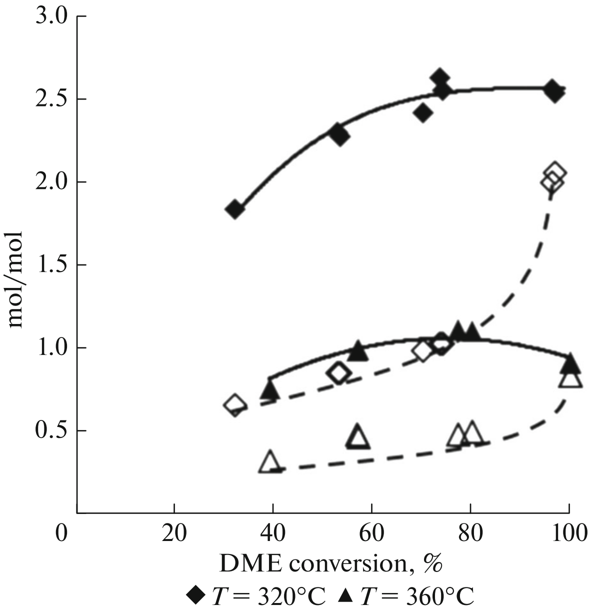

Fig. 9. The C_2H_4/C_3H_6 (dashed line) and C_2H_4/C_4H_8 (solid line) ratio VS DME conversion at the different temperatures.

the contribution of propylene methylation with methanol to form butenes and hydrogen transfer reactions. This assumption is supported by an increase in the selectivity for C_1–C_4 and C_5–C_7 hydrocarbons production with increasing DME conversion. The selectivity for C_5–C_7 hydrocarbons, similar to that of ethylene, decreases production with increasing reaction temperature, while the C_1–C_4 alkane selectivity does not (Fig. 8).

The ratio of the net rates (taking account of the formation and consumption) for the key products can be determined more clearly by analyzing the molar ratios of the product yield. Dependences of the ethylene/propylene and ethylene/butenes yield molar ratio on DME conversion are shown in Fig. 9. With an increase in the reaction temperature, at an identical DME conversion, the ethylene/propylene ratio significantly decreases. Extrapolation of line to the zero DME conversion suggests that, at a high temperature (360°C), ethylene is most probably a product of secondary reactions. In the range of high DME conversion, where the contribution of secondary reactions is significant, the ethylene/propylene ratio abruptly increases; this fact indicates an intensification of the secondary reactions of propylene conversion.

Similarly, at an identical DME conversion, the ethylene/butenes molar ratio also decreases with increasing reaction temperature (Fig. 9). However, in the high DME conversion range, it exhibits a plateau or slightly decreases. Joint analysis of the ethylene/propylene and ethylene/butenes molar ratios suggests that, at high DME conversion, the composition of the resulting products is significantly affected by the propylene methylation reaction. As a consequence, the propylene yield decreases and the butene yield increases.

This conclusion is confirmed by the behavior of the propylene/butenes mole ratio on DME conversion (Fig. 10). At high DME conversion, where secondary reactions occur, the ones ratio is decrease owing to the propylene consumption during methylation reaction with butenes production.

The dependences shown in Fig. 10 exhibit an almost constant propylene/butenes ratio with an increase in the DME conversion to 70–75%, i.e., until the onset of secondary reactions. At a low DME conversion, the total amount of ethylene and butenes in the products is 1 mol per mole of propylene (Fig. 9); with an increase the temperature, at an identical DME conversion, the $C_3H_6/(C_2H_4+C_4H_8)$ ratio increases, although the C_3H_6/C_4H_8 ratio decreases under the same conditions. In this case, the result is attributed to a significant increase in the propylene/ethylene ratio with increasing temperature. In general, the data show that, to achieve a high propylene yield, DME conversion should be run at high temperatures and a minimum contribution of methylation reactions.

The competition of various reactions that occur during DME conversion is clearly revealed by analysis of the ratio between isohydrocarbons and normal

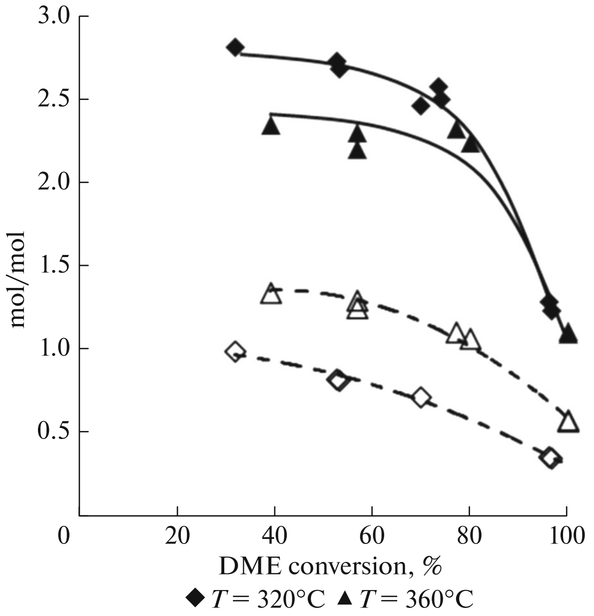

Fig. 10. The C_3H_6/C_4H_8 (solid line) and $C_3H_6/(C_2H_4 + C_4H_8)$ (dashed line) ratio VS DME conversion at the different temperatures.

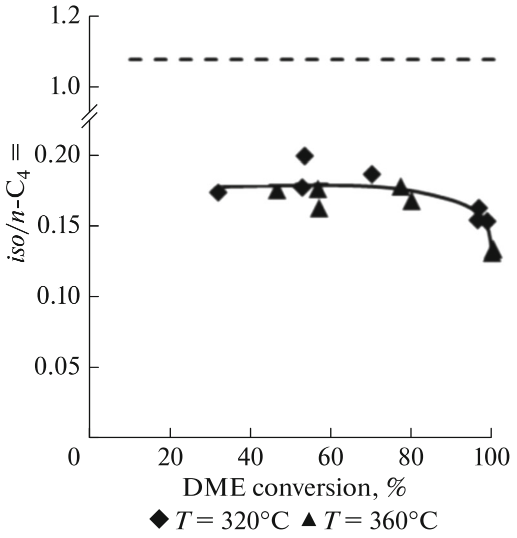

Fig. 11. The isobutenes and *n*-butenes ratio VS DME conversion at the different temperatures (dashed line denotes the thermodynamically equilibrium value).

hydrocarbons in C_4 olefin and alkane fractions (Figs. 11, 12).

It is evident that the *iso-*/*n*-C_4H_8 ratio (Fig. 11) does not depend on the temperature; at a DME conversion up to 70–75%, it is 0.17–0.18; this value is far from the thermodynamically probable value of 0.97–1.08 for the studied temperature range. In the DME conversion range above 75%, the ratio significantly decreases owing to the occurrence of secondary reactions.

The ratio of C_4 isolalkane and *n*-alkane hydrocarbons is up to 9–11; this value is significantly higher than the thermodynamic equilibrium of 0.94–1.05 (Fig. 12). The dependence exhibits a nonmonotonic behavior and increases with the increasing temperature despite the thermodynamic equilibrium suggests the inverse relationship.

Most probably, isobutene, along with other butenes, is a primary product; it is involved in a rapid hydrogen transfer reaction with the predominant formation of isobutane. The isomerization rate of butenes is significantly higher than that of butanes; this feature is responsible for the thermodynamically nonequilibrium content of isobutane in the reaction products. This hypothesis is also confirmed by data on the *trans-*/*cis*-butenes ratio in the reaction products (Fig. 13). This ratio is fairly close to thermodynamic equilibrium; it increases with increasing temperature and approaches a thermodynamic value of 1.3. Thus, it can be assumed that the butenes isomerization rate is sufficient high despite the fact that the rate of butenes formation is considerably higher than that of alkanes.

At high DME conversion rates, the *trans-*/*cis*-butenes ratio abruptly increases and exceeds the thermodynamically equilibrium values; this feature is characteristic of hydrocarbon conversion in the presence of zeolite catalysts by the carbocation mecha-

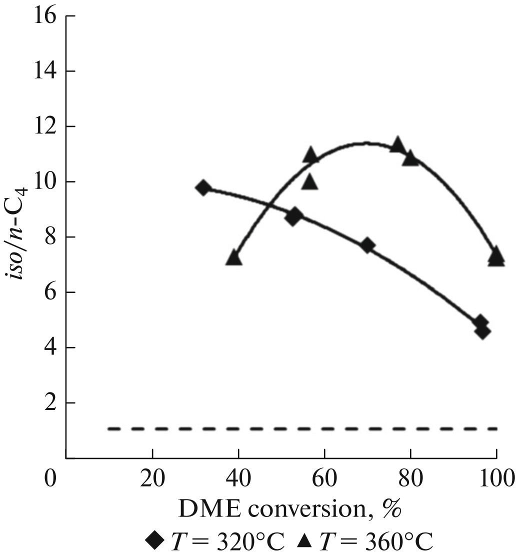

Fig. 12. The isobutanes and *n*-butanes ratio VS DME conversion at the different temperatures (dashed line denotes the thermodynamically equilibrium value).

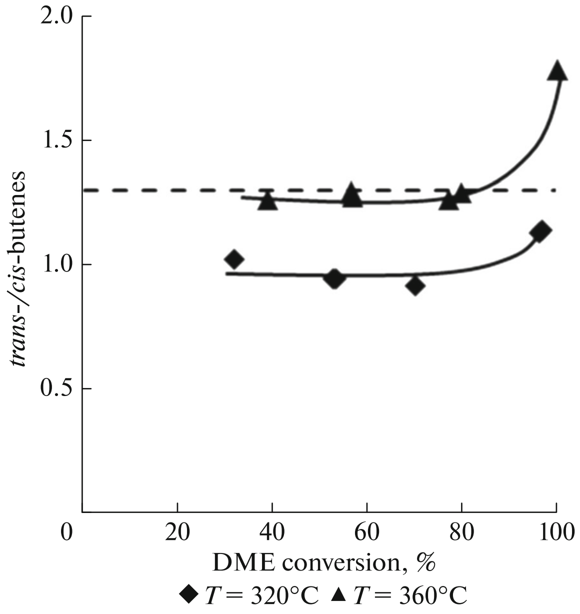

Fig. 13. The *trans*- and *cis*-butenes ratio VS DME conversion at the different temperatures (dashed line denotes the thermodynamically equilibrium value).

nism, which is most likely to occur in secondary reactions involving DME.

Thus, to summarize the data derived in this study, it can be stated that DME conversion over hydrothermal treated Mg–HZSM-5/Al_2O_3 catalyst provides a high methanol yield; the numerical values of the yield pass through a maximum with an increase in the space time. A similar relationship is observed for the propylene yield.

It has been found that the primary products of DME conversion in the presence of this catalyst are methanol, propylene, butenes, and C_5–C_7 hydrocarbons. Ethylene is a primary product at a low reaction temperature and, most probably, a secondary product at a high temperature.

The selectivity of products varies diversely with temperature increasing. The selectivity of methanol and C_1–C_4 alkanes formation does not depend on temperature, while the selectivity of ethylene and C_5–C_7 hydrocarbons decreases with increasing ones. At the same time, the selectivity of propylene and butenes production increases with increasing temperature. The composition of C_2–C_4 olefins formed at a high DME conversion significantly depends on the secondary reactions intensity—methylation and hydrogen transfer—determined by the temperature and the space time.

ACKNOWLEDGMENTS

This work was carried out in the TIPS RAS with support of Russian Science Foundation (project no. 17-73-30046).

REFERENCES

1. U. Olsbye, S. Svelle, M. Bjorgen, et al., Angew. Chem. Int. Ed. **51**, 5810 (2012).
2. M. W. Erichsen, S. Svelle, and U. Olsby, J. Catal. **298**, 94 (2013).
3. D. Lesthaege, J. van der Mynsbrugge, M. Vandichel, et al., Chem. Catal. Chem. **3**, 208 (2011).
4. S. Svelle, P. O. Ronning, and S. Kolboe, J. Catal. **224**, 115 (2004).
5. X. Sun, S. Mueller, H. Shi, et al., J. Catal. **314**, 21 (2014).
6. S. Svelle, P. O. Ronning, U. Olsbye, and S. Kolboe, J. Catal. **234**, 385 (2005).
7. S. Svelle, S. Kolboe, O. Swang, and U. Olsbye, J. Phys. Chem. B **109**, 12874 (2005).
8. S. Svelle, M. Visur, U. Olsbye, and M. Bjorgen, Top. Catal. **54**, 897 (2011).
9. X. Sun, S. Mueller, Y. Liu, et al., J. Catal. **317**, 185 (2014).
10. S. Rabiu and S. Al-Khattaf, Ind. Eng. Chem. Res. **47**, 39 (2008).
11. I. M. Hill, S. A. Hashimi, and A. Bhan, J. Catal. **285**, 115 (2012).
12. I. M. Hill, A. Malek, and A. Bhan, ACS Catal. **3**, 1992 (2013).
13. D. A. Simonetti, R. T. Carr, and E. Iglesia, J. Catal. **285**, 19 (2012).
14. M. Boronat, P. Viruela, and A. A. Corma, J. Phys. Chem. A **102**, 9863 (1998).
15. D. A. Simonetti, J. H. Ahn, and E. Iglesia, Chem. Catal. Chem. **3**, 704 (2011).
16. M. Boronat, P. Viruela, and A. Corma, J. Phys. Chem. B **103**, 7809 (1999).
17. A. T. Aguayo, D. Mier, A. G. Gayubo, et al., Ind. Eng. Chem. Res. **49**, 12371 (2010).
18. P. Kumar, J. W. Thybaut, S. Svelle, et al., Ind. Eng. Chem. Res. **52**, 1491 (2013).
19. H. A. Zaidi and K. K. Pant, Korean J. Chem. Eng. **27**, 1404 (2010).
20. X. Huang, H. Li, W.-D. Xiao, and D. Chen, Chem. Eng. J. **299**, 263 (2016).
21. C. D. Chang and A. J. Silvestri, J. Catal. **47**, 249 (1977).
22. A. S. Al-Dughaither, PhD Dissertation (The University of Western Ontario, 2014).
23. T. S. Zhao, T. Takemoto, and N. Tsubaki, Catal. Commun. **7**, 647 (2006).
24. T. I. Goriyanova, E. N. Biryukova, N. V. Kolesnichenko, and S. N. Khadzhiev, Pet. Chem. **51**, 169 (2011).
25. S. N. Khadzhiev, N. V. Kolesnichenko, E. N. Khivrich, et al., Pet. Chem. **53**, 225 (2013).
26. T. I. Batova, E. N. Khivrich, G. N. Shirobokova, et al., Pet. Chem. **53**, 383 (2013).

27. H. Yamazaki, H. Shima, H. Imai, T. Yokoi, T. Tatsumi, J. N. Kondo, J. Phys. Chem. C, 24091 (2012).
28. P. Perez-Uriarte, A. Ateka, M. Gamero, et al., Ind. Eng. Chem. Res. **55**, 6569 (2016).
29. P. Perez-Uriarte, A. Ateka, A. T. Aguayo, et al., Chem. Eng. J. **302**, 801 (2016).
30. A. Sardesai, T. Tartamella, and S. Lee, Pet. Sci. Technol. **17**, 273 (1999).
31. A. S. Al-Dughaither and H. Lasa, Fuel **138**, 52 (2014).
32. P. Perez-Uriarte, M. Gamero, A. Ateka, et al., Ind. Eng. Chem. Res. **55**, 1513 (2016).
33. A. G. Vlessidisa, L. Nalbandianb, and N. P. Evmiridisa, Microporous Mesoporous Mater. **47**, 369 (2001).
34. L. H. Ong, M. Domok, R. Olindo, et al., Microporous Mesoporous Mater. **164**, 9 (2012).
35. S. M. T. Almutairi, B. Mezari, E. A. Pidko, et al., J. Catal. **307**, 194 (2013).
36. S. M. Campbell, D. M. Bibby, J. M. Coddington, et al., J. Catal. **161**, 338 (1996).
37. S. Zhang, Y. Gong, L. Zhang, et al., Fuel Process. Technol. **129**, 130 (2015).
38. S. N. Khadzhiev, *Catalytic Cracking: Refinery Engineer's Handbook*, Ed. by G. A. Lastovkin, E. D. Radchenko, and M. G. Rudin (Khimiya, Leningrad, 1986) [in Russian].

Translated by M. Timoshinina